

Transmit What You Need: Task-Adaptive Semantic Communications for Visual Information

Jeonghun Park, *Student Member, IEEE*, and Sung Whan Yoon, *Member, IEEE*,

Abstract—Recently, semantic communications have drawn great attention as the groundbreaking concept surpasses the limited capacity of Shannon’s theory. Specifically, semantic communications probably become crucial in realizing visual tasks that demand massive network traffic. Although highly distinctive forms of visual semantics exist for computer vision tasks, a thorough investigation of what visual semantics can be transmitted in time and which one is required for completing different visual tasks has not yet been reported. To this end, we first scrutinize the achievable throughput in transmitting existing visual semantics through the limited wireless communication bandwidth. In addition, we further demonstrate the resulting performance of various visual tasks for each visual semantic. Based on the empirical testing, we suggest a task-adaptive selection of visual semantics is crucial for real-time semantic communications for visual tasks, where we transmit basic semantics (e.g., objects in the given image) for simple visual tasks, such as classification, and richer semantics (e.g., scene graphs) for complex tasks, such as image regeneration. To further improve transmission efficiency, we suggest a filtering method for scene graphs, which drops redundant information in the scene graph, thus allowing the sending of essential semantics for completing the given task. We confirm the efficacy of our task-adaptive semantic communication approach through extensive simulations in wireless channels, showing more than 45 times larger throughput over a naive transmission of original data. Our work can be reproduced at the following source codes: <https://github.com/jhpark2024/jhpark.github.io>

Index Terms—Semantic communications, Communications for computer vision, Scene graphs, Generative models

I. INTRODUCTION

A recent surge in visual applications, which demands substantial traffic, such as virtual and augmented reality, has exacerbated the disparity between the increasing volume of transmitted data and the limited communication capacity [1]–[3]. In this circumstance, the *semantic communication* paradigm has attracted significant interest as a key enabler to break the limit of communication capacity [4]–[7]. In the mid-20th century, the concept of semantic communication was originated by extending Shannon’s classical communication theory to the categorized levels of communications, which acknowledged the required transmission accuracy for the different levels of settings [8]. While Shannon’s original theory primarily focuses on the setting so-called *technical level*, which prioritizes the accurate transmission of raw bits over

a channel, the higher level setting so-called *semantic level* emphasizes not merely the transmission of bits but the delivery of the compressed semantics of the source data, acquiring competitive performance with improved efficiency [9], [10].

The crucial parts of semantic communication include establishing the formal definition of the essential semantics of data and devising the pragmatic extraction methods of compressed semantics from high-dimensional source data. For the definition of semantics, extensive prior research has been conducted to establish the theory of semantic communication [11]–[14]. While each examines subtly distinct concepts, they all share a consistent framework in which source data is encoded into a semantic space at the transmitter side by utilizing the prior knowledge and posterior information of the given data. Although a fundamental concept of the semantic space had been established in the early works, the specific way to represent the extracted semantics was not adequately defined before the machine learning era [9], [11]. Built upon the success of machine learning during the past decade, deep learning (DL) has emerged as a key solution for representing data into the compressed embedding space, which works as a semantic space [15], [16]. The prior research has mainly focused on semantic communications for transmitting visual data. In the next subsection, we provide details of prior efforts in semantic communications for computer vision (CV).

A. Related Works

Semantic Communications for Computer Vision: In the early works of DL-based semantic communication, the joint source-channel coding (JSCC) method was introduced, where it employs convolutional neural networks (CNNs) for extracting a visual semantic, which is the feature vector of a given input image [15], [16]. The DL-based method demonstrates higher compression rates than the traditional image compression techniques while achieving better image reconstruction performance in low signal-to-noise (SNR) and limited bandwidth regimes. Similarly, the cutting-edge model architecture called Transformer [17] is utilized for acquiring rich semantics while surpassing the performance of traditional coding schemes in low SNR conditions [15], [18]. These approaches hold promise for integrating DL-driven methodologies with semantic communication frameworks [9], [19], where the extracted feature is transmitted and then decoded for reconstructing the original data.

Generative Models for Semantic Communications: On the other side, with the substantial progress in deep generative models such as generative adversarial networks (GANs) and

Jeonghun Park and Sung Whan Yoon are with the Graduate School of Artificial Intelligence, Ulsan National Institute of Science and Technology (UNIST), Ulsan 44919, Republic of Korea (e-mail: {jhpark2024, shyoon8}@unist.ac.kr).

Sung Whan Yoon is the corresponding author.

This work has been submitted to the IEEE for possible publication.

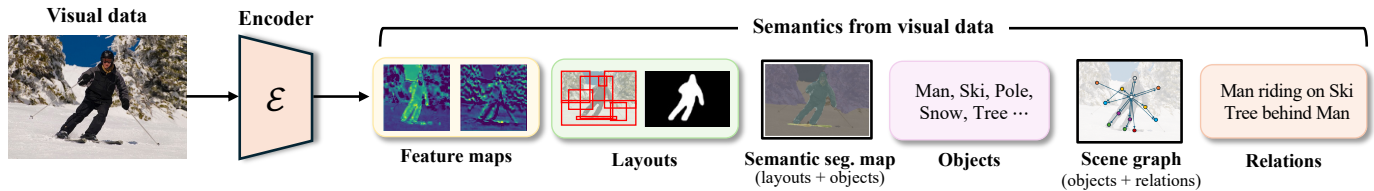


Fig. 1. Semantic features from a given visual data, including feature maps, scene graphs, semantic segmentation maps, layouts, and objects

diffusion models, numerous researchers have explored their applications in semantic communication, especially for visual data reconstruction at the decoder side [20]–[22]. In the cases of [23]–[28], specific semantic features, such as *feature map*, *semantic segmentation map*, and *scene graph (SG)* are extracted from the source image, then used to reconstruct image through the generative models. The reconstructed image is then utilized for CV tasks in some studies [23], [24], [28]. These studies have demonstrated the effectiveness of utilizing semantic features for image transmission and executing CV tasks. For instance, the authors of [27] employed semantic segmentation maps in conjunction with GANs for image transmission, achieving higher compression rates and improved peak signal-to-noise ratio (PSNR) compared to traditional image compression techniques. Built upon this approach, the authors of [23] considered masked feature maps and introduced reinforcement learning (RL) to dynamically adjust the quantization ratio, thereby further reducing the number of transmitted bits. As a different approach, [24] divided the semantic segmentation map into multiple one-hot encode’/;

d maps and applied conventional image compression to them for efficient communication. On the other hand, the authors of [25] leveraged edge maps and textual information, considering the semantic quality and latency constraints. Furthermore, SG-based semantic transmission is explored by employing graph encoding and decoding techniques, outperforming traditional coding schemes [26]. Finally, the authors of [29] also utilized SG while introducing the RL-based method for resource allocations.

Multi-Semantic and Multi-Task: Recently, some prior works have aimed to utilize multiple semantics, including the aforementioned ones, such as semantics semantic segmentation maps and SG. Also, researchers have recently started to consider task-dependent transmission, whose purpose is to transmit task-specific adaptation of semantics. In [30], the authors tackled multi-task scenarios by developing a unified decoder for the multiple semantics. The unified decoder amalgamates the semantic vectors received from the separate encoders, facilitating a cohesive decoding process that efficiently synthesizes information from several source data modalities. In [23], the authors modified the quantization levels of transmitted masked feature maps according to particular CV tasks, including classification, detection, and segmentation.

B. Limitations of Prior Works and Key Motivations

Limitations: While existing studies in generative model-based semantic communication have shown notable efficiency, they primarily focus on a fixed form of semantics without

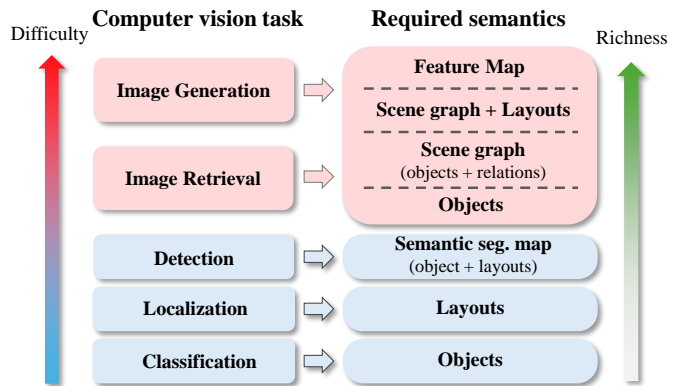


Fig. 2. Task-dependent required semantics for computer vision tasks

considering the target tasks simultaneously. These approaches neglect an important aspect: What are the task-adaptive semantics required to run different CV tasks successfully? The existing methods mostly focus on particular semantics through a semantic encoder and only aim to regenerate the original data through a semantic decoder. They lack a framework to understand task-adaptive semantics for processing different CV tasks. In [23], a quantization level of the masked feature map is adjusted for each task without considering the multiple forms of semantics. Also, in [30], the authors focused on adjusting the number of transmitted feature maps for different tasks. To the best of our knowledge, none of the prior works show a thorough examination of how well the CV tasks are being completed for the different choices of visual semantics while considering transmission throughput and task performance. These limitations increase the communication burden, as extraneous or less relevant semantic information may be transmitted for a given target task.

Semantics of Visual Data: To figure out sufficient information for each task, we illustrate the well-known types of semantic features for a given visual data in Fig. 1. A list of recognized *objects* is the minimal semantics of the given image, e.g., man, ski, pole, etc. Also, *layouts* are in the form of bounding boxes or pixel-wise identifications, which provide localization semantics. When objects and pixel-wise layouts are combined, they form a *semantic segmentation map*, a popular visual semantics used in various CV tasks. As another semantics, *relations* specifies the particular relations or predicates between the recognized objects, e.g., "Man 'riding on' Ski". When objects and relations are combined, they construct a *scene graph*, which describes the recognized objects and their relations. Finally, *feature*

maps are the extracted semantic information that bears overall patterns and spatial information of the given image.

Required Semantics for Different CV Tasks: When we complete a CV task at the receiver side, e.g., a receiver desires to localize the objects captured by the camera at the transmitter side, a transmitter selects proper semantics and sends them to the receiver, e.g., a list of objects and their layouts, which are sufficient for detection, are transmitted. In Fig. 2, we present the scenarios for transmitting semantics to run different tasks, ranging from classification to image regeneration. Also, we elaborate on the details in Section II-B.

C. Contributions

Our key contributions include:

- We have conducted an extensive study of task-adaptive semantic communications for CV tasks that reveals the required semantic features for the given task for accomplishing acceptable performance.
- We propose a semantic feature filtering algorithm, particularly for scene graphs, which aims to minimize semantic redundancy in the scene. This approach maintains the fidelity of the regenerated image while significantly reducing the transmitted data volume.
- We present experimental results demonstrating the effectiveness of the proposed task-adaptive approach in ranging from classification tasks to image generation and retrieval tasks, demonstrating the potential of our approach. Based on the approach, we confirm more than 45 times larger throughput through the efficient selection of visual semantics than a naive transmission of original data in the case of an image generation task.

D. Outlines

Our paper is organized as follows: In Section II, we provide the preliminaries for the further clarification of visual semantics and CV tasks and the basics of diffusion models, which recently work as a semantic decoder. In Section III, the proposed task-adaptive semantic communication is fully described. Next, in Section IV, we present the extensive simulation results to confirm the efficacy of our framework, including the qualitative and quantitative demonstrations in wireless channel settings. Section V concludes the paper.

II. PRELIMINARIES

A. Formulations of Visual Semantics

Let us consider an image sample $\mathbf{x} \in \mathbb{R}^{M \times N}$, where M and N are the width and the length of \mathbf{x} . We then formulate the various visual semantics of the sample as follows:

- **Objects:** These are the individual entities representing tangible items or subjects that can be recognized and classified. As the most fundamental components of an image, objects serve as the building blocks for understanding and interpreting the visual content. We denote the objects as: $\mathcal{O}(\mathbf{x}) = \{o_i\}_{i=1}^I$, where I is the number of objects identified through a semantic encoder. Here, o_i can be an object index or text, such as "Man".

- **Relations:** These semantics capture the interactions and connections between different objects, providing context and understanding of how they relate to one another within the image. These relations often involve structural information that may not be accompanied by a simple layout, providing higher semantic fidelity of the image. As the formula, we denote the relations as: $\mathcal{R}(\mathbf{x}) = \{r_{ij}\}$, where $1 \leq i, j \leq I$ and $i \neq j$. Here, r_{ij} can be a relation index or textual description, such as "riding". Denote $R = |\mathcal{R}(\mathbf{x})|$ as the number of relations.
- **Layouts:** These refer to the spatial arrangement of objects within the image, which plays a crucial role in conveying the overall structure and organization of the image. Examples of layouts include bounding boxes, which delineate the position of objects; edge maps, which highlight the boundaries and contours of objects; and segmentation maps, which provide detailed descriptions of object regions. We formulate layouts as follows: $\mathcal{L}(\mathbf{x}) = \{l_i\}_{i=1}^I$, where $l_i = \{(m, n) \in \mathbb{R}^{M \times N} \mid (m, n) \mapsto o_i\}$. Here, \mapsto indicates that the pixel (m, n) belongs to the object o_i . A layout is a two-dimensional (2D) matrix.
- **Semantic Segmentation Maps:** These indicate the identified objects with their spatial locations. For the formula, we denote the semantic segmentation map as $\mathcal{M}(\mathbf{x}) = \{(o_i, l_i)\}_{i=1}^I$, by simply pairing the objects and layouts.
- **Scene Graphs:** These present the objects and their relations in the form of graphs. We formalize a scene graph as $\mathcal{G}(\mathbf{x}) = \{(V, E)\}$, with its nodes (or vertices) $V = \{v_i\}$ and edges $E = \{e_{ij}\}$. Here, each node indicates each object, i.e., $v_i = o_i$, and each edge corresponds to each relation, i.e., $e_{ij} = r_{ij}$. For another form, we can partition the graph into individual sub-graphs, g_k , corresponding to a pair of nodes (o_i, o_j) and their relation r_{ij} :

$$\mathcal{G}(\mathbf{x}) = \{g_k = (o_i, r_{ij}, o_j) \mid o_i, o_j \in \mathcal{O}, r_{ij} \in \mathcal{R}\}. \quad (1)$$

Here, there exist R individual sub-graphs in $\mathcal{G}(\mathbf{x})$. Each sub-graph can be presented as a sentence, such as "Man is riding on ski".

- **Feature Maps:** These are the representations that entail detailed characteristics and attributes of the image, typically obtained through pretrained deep visual representation models, such as the ResNet architecture [31]. A feature map is a tensor, i.e., $\mathcal{F}(\mathbf{x}) \in \mathbb{R}^{C \times X \times Y}$, where C is the channel size, X and Y are the width and the length of the feature map, as respectively.

B. Scenarios of Visual Tasks

We describe when each computer vision (CV) task is requested and how each task can be accomplished in the communication systems. We assume that a transmitter (Tx) captures visual data \mathbf{x} through a sensor system, such as cameras, and a receiver (Rx) requests a sufficient semantic in order to run a given CV task \mathcal{T} . Here, we drop \mathbf{x} in the notations of semantics for simplicity.

- **Classification:** The Rx hopes to identify the objects from the visual data. In this case, the Tx is sufficient to transmit the recognized objects, i.e., \mathcal{O} , to the Rx.

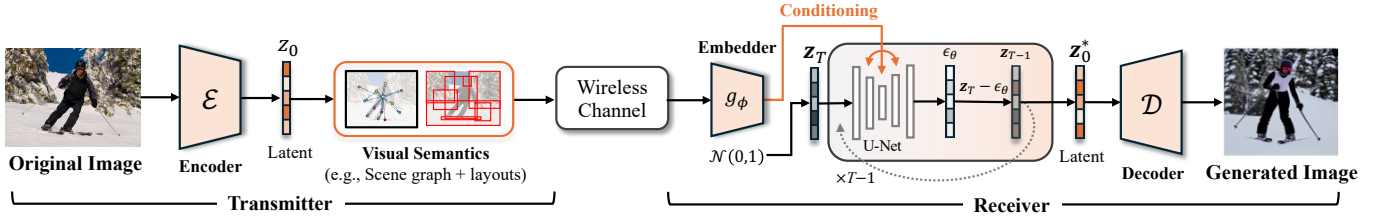


Fig. 3. Image generation task with a latent diffusion model by the conditioning from visual semantics (e.g., a scene graph and layouts)

- **Localization:** The Rx desires to recognize the spatial regions of visual information where some objects are identified. The Tx is then sufficient to transmit the layouts, i.e., \mathcal{L} , to the Rx. As one of the practical scenarios, a vision system that aims to detect the appearance of objects can send the layout to the Rx for localization.
- **Detection:** The Rx wishes to fully detect the objects and their spatial locations. In this case, it is sufficient to transmit the semantic segmentation maps, i.e., \mathcal{M} , or the combination of \mathcal{O} and \mathcal{L} . As a practical scenario, an alert system based on the visual camera at the industrial sites can keep the workers' privacy by not sending full images with their identities but sending the semantic segmentation maps to the Rx.
- **Image Retrieval:** The Rx pursues picking out or retrieving images with semantics similar to the visual information captured on the Tx side. It can be done with simple objects \mathcal{O} , but additional layouts \mathcal{L} possibly add spatial information to it (equivalent to sending semantic seg. maps \mathcal{M}), and relations \mathcal{R} makes the retrieved images more similar to the original one in presenting the relations between objects (equivalent to sending scene graph \mathcal{G}). Finally, the feature map \mathcal{F} provides the full semantic information of the image. As a practical scenario for virtual reality, many portions of visual information do not have to be exactly the same as the original one, but it is sufficient to keep the semantic information the same. In this case, the Tx detours the full image transmission but sends sufficient semantics to run image retrieval.
- **Image Generation:** The Rx aims to regenerate data as identical as possible to the original visual data at the Tx. To this end, objects \mathcal{O} , layouts \mathcal{L} , relations \mathcal{R} , and the feature map \mathcal{F} are possibly needed to be transmitted to the Rx. Richer semantics would be beneficial to accurate regeneration via semantic decoders. The highly accurate replications of visual information, such as Metaverse, can be a practical scenario for image generation.

C. Generative Models in Semantic Communications

In semantic communication systems, generative models are widely utilized to transform compressed semantic features into high-quality visual images, enabling the transmission of only the essential semantic information. In this sense, the generative model itself is often considered as the semantic decoder, serving as a part of the communication system designed to execute tasks [23], [24], [28]. We here present the basics of generative models, particularly in diffusion models, as the

semantic decoder. While various kinds of generative models have been explored in the research field, the diffusion model, known for its outstanding image generation capabilities, has been widely adopted in recent research [24]–[26]. In diffusion models, clean image data is generated from a noise image by gradually removing the additive noise. Thus, the diffusion process is described by the forward process and the reverse process. In the forward process, the original image \mathbf{x}_0 is corrupted by Gaussian noise at each time step $0 < t \leq T$ until it becomes pure noise \mathbf{x}_T . The noised image \mathbf{x}_t at time step t is defined as:

$$q(\mathbf{x}_t | \mathbf{x}_{t-1}) = \mathcal{N}(\mathbf{x}_t; \sqrt{1 - \beta_t} \mathbf{x}_{t-1}, \beta_t \mathbf{I}), \quad (2)$$

where $\mathcal{N}(\cdot; \mu, \sigma^2)$ is the Gaussian distribution of mean μ and variance σ^2 . In the reverse process, starting from \mathbf{x}_T , the model parameterized with θ to estimate the error, i.e., ϵ_θ , iteratively denoises the image by simply predicting the added noise at each time step [22]. The loss is for minimizing the difference between the true noise ϵ and the predicted noise ϵ_θ :

$$L := \mathbb{E}_{t, \mathbf{x}_0, \epsilon} [|\epsilon - \epsilon_\theta(\mathbf{x}_t, t)|^2]. \quad (3)$$

For a more efficient diffusion process, the latent diffusion model (LDM) was proposed [32]. Instead of applying the diffusion process directly in pixel space, LDM performs diffusion in a lower-dimensional latent space learned by a pretrained VAE. By using a latent representation of the data, i.e., \mathbf{z}_t , the model can focus on the essential semantics of the image, allowing faster and more efficient generation without sacrificing quality. In addition to its efficiency, it is capable of generating images conditioned on a variety of semantic information. The loss function of LDM-based conditioning is expressed as:

$$L_{\text{LDM}} := \mathbb{E}_{t, \mathbf{y}, \epsilon} [|\epsilon - \epsilon_\theta(\mathbf{z}_t, t, g_\phi(\mathbf{y}))|^2], \quad (4)$$

where \mathbf{y} corresponds to the conditions and g_ϕ embeds the conditions to the latent space. In Fig. 3, we further envision how the conditioned generation of LDM can be used in semantic communications, where the received semantics are used as conditioning. When the Tx transmits a scene graph, i.e., \mathcal{G} , and layouts, i.e., \mathcal{L} , the Rx utilizes the semantics as the conditioning to be injected into the diffusion process through the attention layers of the U-Net, guiding the denoising process to ensure the generated image aligns with the given condition.

III. PROPOSED TASK-ADAPTIVE SEMANTIC COMMUNICATION SYSTEMS

In this section, we provide a full description of our proposed semantic communication systems for computer vision (CV)

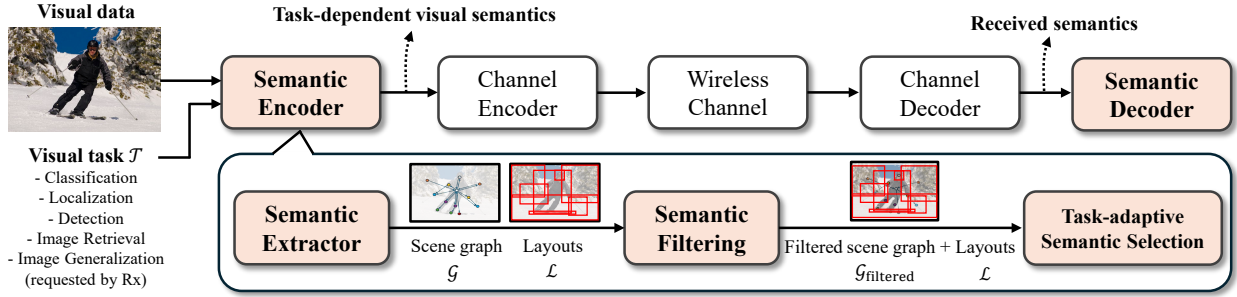


Fig. 4. The proposed framework of the semantic encoder part. Here, we illustrate the case of transmitting the scene graphs, i.e., \mathcal{G} (objects + relations), and the layouts, i.e., \mathcal{L} . After filtering out redundant sub-graphs to obtain $\mathcal{G}_{\text{filtered}}$, the encoder sends the selected semantics through the wireless channel.

tasks. As aforementioned in Section II, our communication scenario is initiated as follows: For a given pair of a transmitter (Tx) and a receiver (Rx), the Rx aims to complete a certain CV task for the given visual data at the Tx side, and it requests the semantic information of the data.

First, the Tx begins to process to obtain the proper visual semantics of the data, which is tailored to complete the requested CV task by the Rx. Specifically, Fig. 4 illustrates the process, particularly for the *semantic encoder* part of the Tx. Semantic Encoder consists of three main blocks: **i)** Semantic extractor block, **ii)** Semantic filtering block, and **iii)** Task-adaptive semantic selection block.

The semantic extractor block is for extracting semantic features from the input image. As listed in part II-A, the semantic extractor is capable of obtaining objects, i.e., \mathcal{O} , layouts, i.e., \mathcal{L} , relations, i.e., \mathcal{R} , semantic segmentation maps (objects + layouts), i.e., \mathcal{M} , scene graphs (objects + relations), i.e., \mathcal{G} , and feature maps, i.e., \mathcal{F} .

The semantic filtering block filters the semantics for dropping less informative or redundant information. In the extracted semantics, some are trivial, so thus less informative, or some are inferable from others, so thus redundant. Here, we focus on filtering a scene graph, which yields a significant gain in transmission efficiency without losing utility.

Finally, the task-adaptive semantic selection block ensures that only the semantic features required for the CV task are transmitted. The selection process is guided by the specific requirements of the target task, and in some cases, task performance considerations are also factored into selection.

We further provide detailed explanations of each block, highlighting their roles and contributions to our framework.

A. Semantic Extractor

For a given image \mathbf{x} , the semantic extractor block begins with obtaining the feature map, i.e., $\mathcal{F}(\mathbf{x})$ through a feature extractor architecture. In our system, we utilize the ResNet architecture as the feature extractor for the experiments, but it is not limited to using the particular model architecture [32].

From the feature map, as mostly done by vision models, the following semantics are computed: Objects $\mathcal{O}(\mathbf{x})$, Layouts $\mathcal{L}(\mathbf{x})$, and Relations $\mathcal{R}(\mathbf{x})$. In our framework, we use the Transformer architecture to acquire the aforementioned semantics, which is the cutting-edge method for computing

visual semantics. Also, layouts can be the forms of bounding boxes or pixel-wise layouts. In our experiments, we utilize the bounding box form for a more compact transmission.

Based on the obtained semantics, the semantic segmentation maps, i.e., $\mathcal{M}(\mathbf{x})$, can be computed by simply using the objects and the pixel-wise layouts.

In addition, the scene graph, i.e., $\mathcal{G}(\mathbf{x})$, is computed by combining the objects and the relations by following the scene graph generation process in [33]. Each node is assigned to each object, and each edge corresponds to each relation, as formulated in Section II-A. For further processing, the graph can be transformed into a set of sub-graphs by following Eq. (1). By partitioning $\mathcal{G}(\mathbf{x})$ into an individual sub-graph, i.e., g_k , each sub-graph can be represented with a sentence about two objects, o_i , o_j , and their relation r_{ij} .

B. Semantic Filtering

For the extracted visual semantics, our framework compresses them by filtering out less informative or redundant information. For layouts, it is hard to filter out them because the layouts are the only semantics bearing spatial information. Also, objects and relations present the categories of recognized objects and their relations, which contain non-overlapping information. For other semantics, such as feature maps and semantic segmentation maps, prior methods exist to mask them to compress the information.

On the other hand, we here focus on scene graphs, which combine objects and relations, containing less-informative or redundant sub-graphs that can be dropped in transmission. The probability of the scene graph \mathcal{G} is:

$$\mathbb{P}(\mathcal{G}) = \mathbb{P}(g_1, g_2, \dots, g_K) = \prod_{k=1}^K \mathbb{P}(g_k | g_1, \dots, g_{k-1}). \quad (5)$$

Based on the probability formulation, we here consider two scenarios for filtering: less informative and redundant cases.

Less Informative Relations Filtering: Assuming that the probability of observing each object in an image is independent, the probability of sentence or sub-graph g_k is:

$$\mathbb{P}(g_k) = \mathbb{P}(o_i, r_{ij}, o_j) = \mathbb{P}(r_{ij} | o_i, o_j) \cdot \mathbb{P}(o_i) \cdot \mathbb{P}(o_j). \quad (6)$$

We can drop the relation (edge of graph), which carries low information content: $\mathbb{P}(r_{ij} | o_i, o_j) \approx 1$. Note that it does not represent the marginal probability, i.e., $\mathbb{P}(r_{ij})$, but

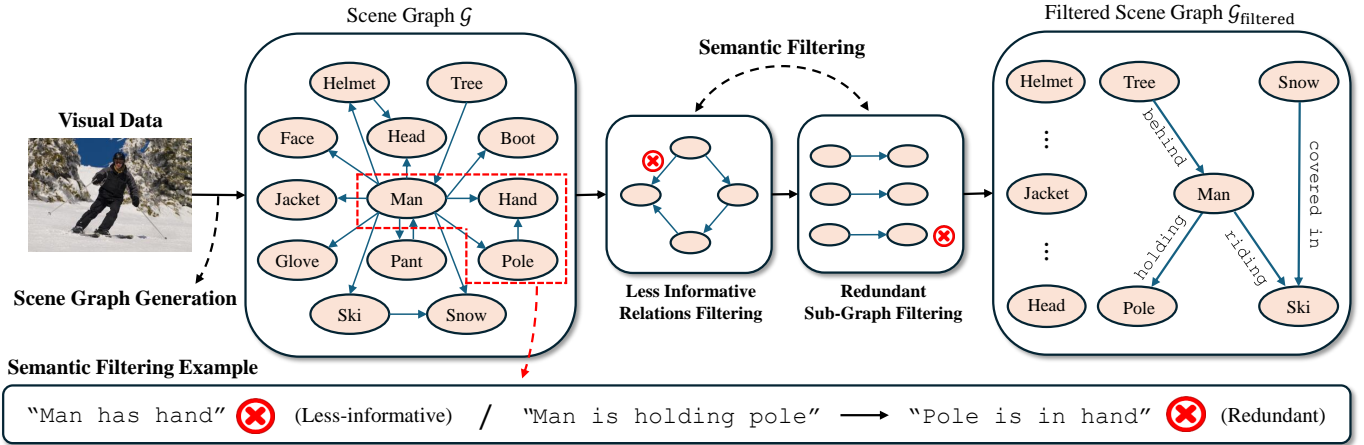


Fig. 5. Semantic Filtering

Algorithm 1 Less Informative Relations Filtering Algorithm**Require:** A scene graph $\mathcal{G} = \{g_k\}$, threshold $0 \leq \tau_f \leq 1$ **Ensure:** A filtered scene graph $\mathcal{G}_{\text{filtered}}$

- 1: Initialize $\mathcal{G}_{\text{filtered}} \leftarrow \mathcal{G}$
- 2: **for** each sentence $g_k = (o_i, r_{ij}, o_j) \in \mathcal{G}$ **do**
- 3: Compute $\mathbb{P}(r_{ij} | o_i, o_j)$
- 4: **if** $\mathbb{P}(r_{ij} | o_i, o_j) \geq \tau$ **then**
- 5: Remove r_{ij} from $\mathcal{G}_{\text{filtered}}$
- 6: **end if**
- 7: **end for**
- 8: **return** $\mathcal{G}_{\text{filtered}}$

the conditional probability of r_{ij} , given two objects o_i and o_j . For instance, when a "man has head" is detected in the image, the conditional probability of the relation "has" approximates to 1, indicating that the relation carries low information. On the contrary, let us consider another example of "cat wearing hat". If the sender has rarely observed a cat wearing a hat, the conditional probability of the relation "wearing" would be low, suggesting that this observation carries a high amount of information, regardless of how explicit or obvious the relationship appears. Thus, the semantic featuring block drops r_{ij} with sufficiently large conditional probability¹, as described in Algorithm 1.

Redundant Sub-Graph Filtering: Next, we can further compress scene graphs by filtering out redundant sub-graphs. When a sub-graph or sentence g_k is trivially inferred with given other sub-graphs, i.e., $\mathbb{P}(g_k | g_1, \dots, g_{k-1}) \approx 1$, then g_k does not need to be transmitted. Let us go back to Fig. 5. We can trivially infer a sub-graph or sentence "Pole is in hand" given "Man is holding pole". It shows a sub-graph provides sufficient information to infer another sub-graph. For this case, we can filter out "Pole is in hand" by selecting "Man is holding pole". In another case, multiple sub-graphs can be used together to infer another one. For example, with the combination of "man is riding

horse" and 'tree is behind man', we can trivially infer "tree is behind horse".

However, there remains a critical challenge to formalizing the steps to filter out inferable sub-graphs. In the aforementioned cases, humans easily figure out the redundant one based on common sense: Man often holds something with their hands, and the horse with man is behind the tree because the man is behind it. To utilize the in-depth semantics behind each sub-graph, we leverage a pretrained language model, such as Sentence-BERT (S-BERT) in [34], to recognize redundant sentences. As with other recent language models, the key characteristic of S-BERT is its ability to encode sentences or phrases into dense embedding vectors so that the relationships between them can be measured effectively. In particular, when two embedding vectors represent semantically entailing sentences, the cosine similarity or Euclidean distance between them becomes minimal. On the other hand, if the sentences are in a contradictory relationship, these metrics yield larger distances. In cases where the relation is neutral, the vectors are close to being perpendicular in the vector space. Based on this property, the conditional probability of a sentence g_k based on others can be well-estimated.

When embedding our sub-graph sentence g_k via a language model $F_{\text{LM}}(\cdot)$, the normalized embedded vector is denoted as $\mathbf{g}_k := F_{\text{LM}}(g_k) / \|F_{\text{LM}}(g_k)\|$. Let us then consider a case with three vectors $\mathbf{g}_1, \mathbf{g}_2, \mathbf{g}_3$ from g_1, g_2, g_3 , respectively. When subtracting the direction of \mathbf{g}_3 from the other two via projection, the following are obtained:

$$\mathbf{g}_{1|3} = \mathbf{g}_1 - \text{Proj}_{\mathbf{g}_3}(\mathbf{g}_1) \quad (7)$$

$$\mathbf{g}_{2|3} = \mathbf{g}_2 - \text{Proj}_{\mathbf{g}_3}(\mathbf{g}_2), \quad (8)$$

where $\text{Proj}_{\mathbf{u}}(\mathbf{v})$ is the projected \mathbf{v} on \mathbf{u} . The process removes the information of \mathbf{g}_3 from the other two vectors. From the view of \mathbf{g}_1 , when further subtracting the information of \mathbf{g}_2 , we can solely focus on the residual vector, i.e., \mathbf{r}_1 , of \mathbf{g}_1 :

$$\mathbf{r}_1 := \mathbf{g}_{1|2,3} = \mathbf{g}_{1|3} - \text{Proj}_{\mathbf{g}_2}(\mathbf{g}_{1|3}) \quad (9)$$

$$= \mathbf{g}_{1|3} - \text{Proj}_{\mathbf{g}_{2|3}}(\mathbf{g}_{1|3}). \quad (10)$$

¹In experiments, we compute it based on the frequency to appear r_{ij} given o_i and o_j , in a given dataset or knowledge base.

Algorithm 2 Redundant Sub-Graph Filtering Algorithm

Require: A set of vectors $\mathcal{G}_{\text{LM}} = \{\mathbf{g}_k\}$, threshold $0 \leq \tau_r \leq 1$

Ensure: Filtered scene graph $\mathcal{G}_{\text{filtered}}$

```

1: while True do
2:   for each  $\mathbf{g}_k \in \mathcal{G}_{\text{LM}}$  do
3:     for each  $\mathbf{g}_j \in \mathcal{G}_{\text{LM}}$  do
4:       if  $j \neq k$  then
5:         Remove information from vector :
            $\mathbf{g}_{k|[j]\setminus k} \leftarrow \mathbf{g}_{k|[j-1]\setminus k} - \text{Proj}_{\mathbf{g}_j}(\mathbf{g}_{k|[j-1]\setminus k})$ 
6:       end if
7:     end for
8:     Compute the Euclidean norm of the residual vector:
            $\|\mathbf{r}_k\| \leftarrow \|\mathbf{g}_{k|[K]\setminus k}\|$ 
9:   end for
10:  Find  $\mathbf{r}_m$  with the smallest Euclidean norm.
11:  if  $\|\mathbf{r}_m\| < \tau_r$  then
12:    Remove  $\mathbf{g}_m$  from  $\mathcal{G}_{\text{LM}}$ 
13:  else
14:    break
15:  end if
16: end while
17:  $\mathcal{G}_{\text{filtered}} \leftarrow \{\mathbf{g}_k \mid \mathbf{g}_k \in \mathcal{G}_{\text{LM}}\}$ 
18: return  $\mathcal{G}_{\text{filtered}}$ 

```

When the Euclidean norm, i.e., $\|\mathbf{g}_{1|2,3}\|$ gets close to zero, g_2 , g_3 or combination of them entails the meaning of g_1 , which can be interpreted as g_1 can be inferred from other sentences i.e., $\mathbb{P}(g_1 \mid g_2, g_3) \approx 1$. In other words, g_1 is semantically redundant. As a general form of residual vector: $\mathbf{r}_k = \mathbf{g}_{k|[K]\setminus k}$, where $[K]$ indicates a set of integers less than or equal to K . Algorithm 2 presents the generalized form of this approach to identify and filter out semantically redundant features systematically. We denote the set of normalized embedded vectors of sentences $\{g_k\}$ as follows:

$$\mathcal{G}_{\text{LM}} = \left\{ \mathbf{g}_k = \frac{F_{\text{LM}}(g_k)}{\|F_{\text{LM}}(g_k)\|} \mid g_k \in \mathcal{G} \right\}. \quad (11)$$

Fig. 5 illustrates the steps to obtain the filtered scene graph.

C. Task-Adaptive Semantic Selection

Our approach identifies the semantic features needed for each task and transmits them accordingly. The required semantic features of each task are illustrated in Fig. 2. Also, we fully describe the scenarios of each visual task in Section II-B to elaborate on the required semantics for each task.

Based on the understanding, our system provides a set of visual semantics, including objects $\mathcal{O}(\mathbf{x})$, layouts $\mathcal{L}(\mathbf{x})$, semantic segmentation maps $\mathcal{M}(\mathbf{x})$, filtered scene graphs $\mathcal{G}_{\text{filtered}}(\mathbf{x})$, and feature map $\mathcal{F}(\mathbf{x})$ enabling task-adaptive selection of them.

IV. EXPERIMENTAL RESULTS

The experiments of our framework are threefold: **i)** evaluation of task performance to show how much a given visual task is performed well, particularly for the most challenging cases,

i.e., image generation and retrieval, **ii)** demonstration on wireless communication channels to confirm how fast processing of a given visual task is possible, **iii)** Analysis of end-to-end latency for the overall process to verify real-time working. Specifically, we first analyze the task performance across various scenarios where different tasks are required, focusing on how the selection of different semantic features impacts the results. We then evaluate the communication efficiency achieved through the selective and efficient transmission of semantic features on wireless channels. Lastly, we analyze end-to-end latency for varying tasks to evaluate the real-time working availability of our proposed framework.

A. Experimental Settings

Datasets: In the experiments, two different visual datasets are used: the Visual Genome dataset and the COCO dataset [35], [36]. A brief description and their usages are as follows.

- **Visual Genome Dataset [35]:** This dataset was used for image generation and image retrieval tasks. It consists of images annotated with detailed information, such as objects and relationships, making it well-suited for semantic feature extraction and assessing the effectiveness of our system in generating or retrieving images based on semantic features.
- **COCO Dataset [36]:** For image classification, localization, and detection, we use the subset of the COCO dataset. It is widely used for various CV tasks and serves as a popular standard benchmark.

Model Architectures: For the semantic extractor, we employ the ResNet-50 encoder [32] that transforms a given image $\mathbf{x} \in \mathbb{R}^{3 \times M \times N}$ to the feature map, i.e., $\mathcal{F}(\mathbf{x}) \in \mathbb{R}^{C \times X \times Y}$. The encoder is pretrained on ImageNet-1K classification task [37]. Specifically in our configuration, $M = N = 512$, and $X = Y = 16$. The channel dimension C is 2048. To obtain semantic features described in II, the overall process is as follows: First, we utilize a transformer encoder-decoder architecture to obtain $\mathcal{O}(\mathbf{x})$ and $\mathcal{L}(\mathbf{x})$ from $\mathcal{F}(\mathbf{x})$. However, as $\mathcal{F}(\mathbf{x})$ it has a high-dimensional channel space, which is less suitable for transformer architecture, 1×1 convolution is applied $\mathcal{F}(\mathbf{x})$ to reduce channel dimensions C to smaller $d = 256$. Then, the feature map is flattened resulting $\mathcal{F}_0(\mathbf{x}) \in \mathbb{R}^{d \times XY}$. To encode spatial information, we add a fixed positional embedding $E_p \in \mathbb{R}^{d \times XY}$ to the feature map resulting $\mathcal{F}_p(\mathbf{x})$. The encoder part utilizes a self-attention layer to obtain a context-aware feature $\mathcal{F}_c(\mathbf{x}) \in \mathbb{R}^{d \times XY}$ from $\mathcal{F}_p(\mathbf{x})$. Then, the decoder part introduces a set of $N_o = 100$ learnable object queries designed to represent a potential object within the image, allowing the model to focus on specific parts of the image relevant to individual objects. In this sense, the cross-attention stage utilizes object queries $\mathcal{F}_c(\mathbf{x})$ to generate object representation vectors. In our configuration, we utilize 6 encoder and 6 decoder layers with the number of heads 8. Finally, each object representation can be used to predict $\mathcal{O}(\mathbf{x})$, and $\mathcal{L}(\mathbf{x})$, i.e., a bounding box, through feed-forward networks. For this process, we utilized a model in [38], which is trained on COCO detection task.

Obtaining $\mathcal{R}(\mathbf{x})$ from $\mathcal{F}(\mathbf{x})$ is fundamentally similar to the above method but requires a few distinct steps. First, it utilizes two separate branches for decoding, considering the fact that relation inherently involves two distinct objects and is sensitive to order; for example, "man riding ski" and "ski riding man" describe different relationships. In this sense, each branch utilizes distinctive $N_r = 200$ learnable object queries $Q_{o1} \in \mathbb{R}^{d \times N_r}$ and $Q_{o2} \in \mathbb{R}^{d \times N_r}$. Also, different object embeddings $E_{o1} \in \mathbb{R}^{d \times N_r}$ and $E_{o2} \in \mathbb{R}^{d \times N_r}$ are added to each object query. Here N_r is a number of object pairs that are considered. Lastly, learnable relation embedding $E_r \in \mathbb{R}^{d \times N_t}$ is added to object queries on both branches. Thus, the resulting queries in each branch are expressed as: $Q_1 = Q_{o1} + E_{o1} + E_r$, $Q_2 = Q_{o2} + E_{o2} + E_r$. However, the object queries do not yet incorporate the context from the visual data. To address this, we concatenate these two queries and pass them through a self-attention layer. In this setup, we set $Q = K = [Q_1, Q_2]$, and $V = [Q_{o1}, Q_{o2}]$ where $[\]$ indicates the concatenation process. This encoding process allows the model to consider the relational context between the objects represented by each query. The output of the encoder is decoupled to continue the decoding process in each branch, and the following procedure is similar to the aforementioned process. Each branch obtains object representation through the cross attention with $\mathcal{F}_c(\mathbf{x})$ and utilizes feed-forward networks merging the outputs of two branches to predict $\mathcal{R}(\mathbf{x})$. Here, we utilize a model architecture with 6 encoder and 6 decoder layers, each with 8 attention heads. Finally, with a combination of $\mathcal{O}(\mathbf{x})$ and $\mathcal{R}(\mathbf{x})$, a scene graph $\mathcal{G}(\mathbf{x})$ is achieved. For this process, we adopted a model in [33], which is trained on Visual Genome dataset. The object classes total 151, and the relation classes total 51. As depicted in 3, by utilizing extracted semantic features i.e., $\mathcal{O}, \mathcal{L}, \mathcal{M}, \mathcal{R}$, and \mathcal{G} , a semantically aligned image can be generated by LDM following [38].

For feature map-based image generation, an iterative denoising process conditioned on $\mathcal{F}(\mathbf{x})$ might be inefficient in terms of both communicational burden and latency. Instead, a feature map $\mathcal{F}_d(\mathbf{x}) \in \mathbb{R}^{C_d \times X_d \times Y_d}$ that can be directly decoded into the image can be used. So, we additionally adopt an encoder, i.e., a feature map extractor, which pairs to the decoder of the receiver. Specifically the encoder consists of residual blocks which down-samples \mathbf{x} into $\mathcal{F}_d(\mathbf{x})$ while decoder up-samples it and resulting $\mathbf{x}^* \in \mathbb{R}^{3 \times M \times N}$. In our configuration, $X_d = Y_d = 64$ and $C_d = 4$.

We freeze all the pretrained model parameters without requiring further training. All implementation source codes are provided in <https://github.com/jhark2024/jhark.github.io>.

Hyperparameters for Algorithm 1 and 2: Through exhaustive search, we found the thresholds in the algorithms for filtering scene graphs: $\tau_f = \tau_r = 0.8$, respectively. To filter less informative relations, we computed the probability of observing objects and relations using scene graph generation on 100,000 images from the Visual Genome dataset.

B. Task Performance Evaluation

Herein, two tasks are primarily considered: image generation and image retrieval, which are the most challenge ones.

TABLE I
PERFORMANCE OF IMAGE GENERATION ON VISUAL GENOME DATASET

Semantic Features	CLIP Similarity \uparrow	Pixel L2 \downarrow
Feature Map (comp. rate 0.020)	0.963	39.9
Feature Map (comp. rate 0.008)	0.806	82.3
SG + Layout	0.856	145.1
Filtered SG + Layout	0.856	145.0
Object + Layout	0.855	145.5
Sem. Seg. Map	0.841	140.3
SG	0.832	147.6
Filtered SG	0.832	147.9
Object	0.824	148.2

\uparrow : higher is better, \downarrow : lower is better, SG: Scene Graph, i.e., \mathcal{G} , Filtered SG: Filtered Scene Graph, i.e., $\mathcal{G}_{\text{filtered}}$, comp. rate: Compression rate

For simpler tasks, classification is completed by sending $\mathcal{O}(\mathbf{x})$, localization is done by sending $\mathcal{L}(\mathbf{x})$, and detection is finished by transmitting a pair of $\mathcal{O}(\mathbf{x})$ and $\mathcal{L}(\mathbf{x})$ or semantic segmentation map $\mathcal{M}(\mathbf{x})$. Thus, we have excluded these simpler tasks from our analysis here.

Image Generation Task: Fig. 3, illustrates the process of image generation. We use two different metrics for evaluating image generation. As the performance metric for quantitative results, we use CLIP cosine similarity to measure semantic similarity at a fine-grained level [39]. Fréchet Inception Distance (FID), which shows the overall similarity of the original and generated data distributions, is not suitable to our case, which assesses the sample-wise similarity. In contrast, a CLIP model utilizes a text-vision embedding space that captures high-level semantic information, making it more suitable for evaluating semantic alignment.

For a more strict metric for confirming how much the generated one is identical to the original one, i.e., a pixel-wise L2 distance. We measure the pixel-wise L2 distance between the pair of original and generated images. When measuring L2 distance, we resize both the original image and generated image to have the size 224×224 .

Table I presents the evaluation results of image generation tasks when using different visual semantics. Considering the randomness of the generating process due to the sampling process of the diffusion model, the results are averaged on testing 3,000 images. The results indicate that utilizing more diverse semantic information leads to higher performance on both two metrics, with a particularly significant improvement observed when incorporating layout information. When comparing 'Sem. Seg. Map' and 'Object + Layout', despite 'Sem. Seg. Map' delivers more detailed layout information that contributes to achieving lower pixel-wise error; it struggled to generate semantically similar images for scenes with complex arrangements. More importantly, our proposed semantic filtering algorithm shows minimal degradations, while the filtered scene graph (SG) uses approximately one-third of the full graph, demonstrating that the proposed algorithm effectively eliminates less informative and semantically redundant features. The transmission efficiency is analyzed afterward.

To provide a qualitative analysis, we include examples of



Fig. 6. The qualitative results of the image generation task for Visual Genome. A given original image is regenerated via sending different visual semantics.

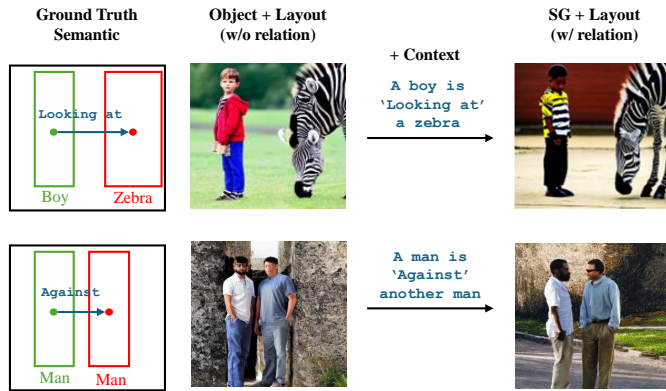


Fig. 7. The qualitative effects of the relations in the image generation task.

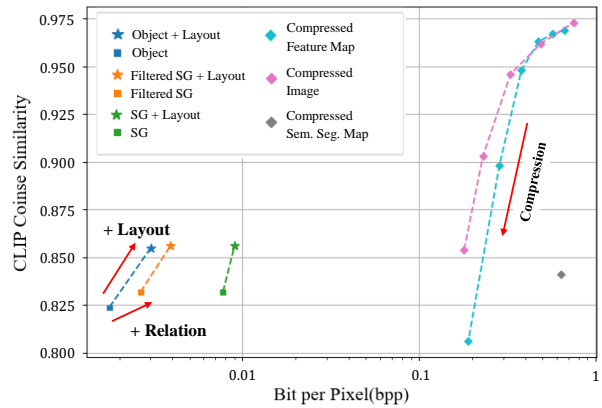


Fig. 8. CLIP cosine similarity v.s. bit per pixel for the image generation task

the generated images in Fig. 6 to visualize the generated results from different semantics. Starting with the images generated using only object information, it is observed that while the objects appear in the scene, the generated images struggle to capture the context in cases where the relationships between objects are crucial. In contrast, as SG incorporates relation information, the generated images better reflect the contextual relationships among the objects, resulting in more coherent scenes. However, there is still a noticeable difference in the composition of the images. This issue is effectively addressed by adding simple layout information, such as bounding boxes. The three examples on the right in Fig. 6 show that incorporating layout information significantly enhances the semantic similarity of the generated images, allowing the model to produce images that are much semantically closer to the original. This improvement can be attributed to the fact that the combination of layout and object information allows the model to infer certain spatial relationships that correlate with the given relations, leveraging the statistical knowledge

embedded in the generative model.

Let us focus on the benefits of sending relations. Fig. 7 illustrates a case where the inclusion of relation information is crucial in generating semantically accurate images. The example in the figure shows where incorporating relation information helps capture the scene’s context.

We emphasize that our semantic filtering block identifies the crucial relations that largely affect the visual semantics. Thus, the important relations are kept to be transmitted.

Fig. 8 illustrates the relationship between bit per pixel (bpp) and CLIP cosine similarity based on the type of semantic features and its fidelity. A smaller bpp means that fewer bits are required to transmit information. For ‘Compressed Image,’ the conventional compression method, i.e., JPEG, is applied. For the feature map, we compressed it with different quantization levels, which is a commonly adopted method for feature map compression [23]. The result shows that compressed images and feature map quickly degrade their similarity with a higher compression rate. When the bpp gets close to 0.1,

TABLE III
SYSTEM PARAMETERS OF WIRELESS COMMUNICATIONS EXPERIMENTS

Parameters	Values
Channel bandwidth	5 MHz
Subcarrier spacing	15 KHz
Modulation	QPSK
Source coding A*	JPEG (image)
Source coding B†	ASCII (text)
Channel coding	LDPC (base graph 1)
Codeword length A*	8448
Codeword length B†	1056
Code rate	(1/3), (1/2), (2/3), (5/6)
Decoding Iteration	20

*: ‘Source coding A’ and ‘Codeword length A’ are for images, feature maps, and semantic segmentation maps.

†: ‘Source coding Type B’ and ‘Codeword length B’ are for objects, relations, layouts, and scene graphs.

can further accelerate the transmission, where ‘Filtered SG’ shows 3 times larger throughput than ‘SG’.

For a naive transmission of images, merely one image transmission per second is achievable in low-SNR conditions for the compressed version, emphasizing that real-time transmission is infeasible. In contrast, transmitting filtered scene graph and layout information, i.e., ‘Filtered SG + Layout,’ enables sending hundreds of images per second even at 0 dB SNR. These results suggest that in scenarios with limited bandwidth, transmitting highly compressed semantic features is crucial for supporting real-time vision tasks.

D. Estimation of End-to-End Latency

Latency Terms: Beyond confirming the reduced transmission time for our task-adaptive semantics in Sec. IV-C, the overall end-to-end latency, including the semantic encoding at the transmitter, transmission through the channel, and the completion of the visual task at the receiver, should be considered to verify the practicality of this system. The resulting overall latency is obtained by summing all terms:

$$\tau_{\text{total}} \approx \tau_{\text{se}} + \tau_{\text{ce}} + \tau_{\text{tx}} + \tau_{\text{cd}} + \tau_{\text{task}}. \quad (12)$$

The first factor τ_{se} represents the time required to extract visual semantics from an image, i.e., semantic encoding. In our work, the semantic extractor relies on deep model architecture, e.g., ResNet-50 and auxiliary networks. The latency encompasses the inference time of the semantic extractors.

The second factor τ_{ce} is channel coding time, especially LDPC coding in our configuration. However, τ_{ce} is negligibly small compared to other components, so we assume $\tau_{\text{ce}} = 0$ during latency measure.

The third factor τ_{tx} is transmission latency, which is determined by channel conditions, available communication resources, and the compression level of semantic features. As shown in Fig. 10, different semantics show largely different transmission latency.

The fourth factor τ_{de} is channel decoding time. Contrary to channel coding time, τ_{de} can be substantially large as a

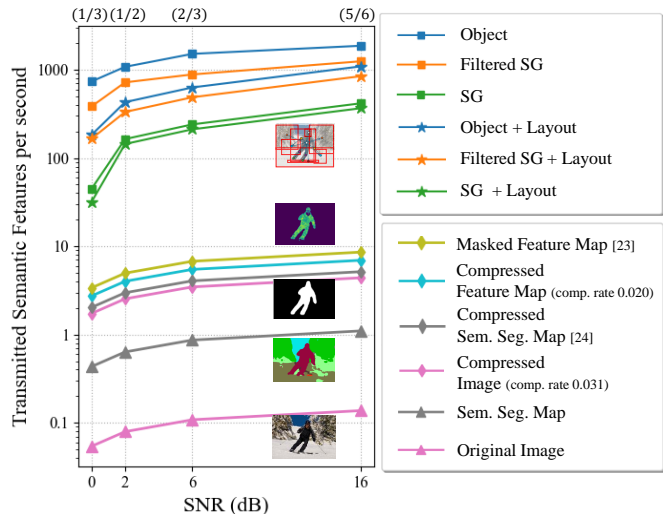


Fig. 10. The transmission throughput of different types of visual semantics on wireless communication channels, based on the Visual Genome Dataset

LDPC code requires iterative decoding. However, τ_{de} can be significantly reduced when parallelized computing is available. In other words, fast delivery of semantic features, i.e., small $\tau_{\text{se}} + \tau_{\text{ce}} + \tau_{\text{tx}}$ can potentially reduce τ_{de} per image.

The final factor τ_{task} , is the required time to complete the vision task based on the decoded data. This component can largely vary depending on the representation received data and the task type. As described in Sec. II-B, a group of simple tasks, such as classification, localization, and detection, can be completed right after receiving \mathcal{O} , \mathcal{L} , and \mathcal{M} (or \mathcal{O} plus \mathcal{L}), respectively, thus not requiring τ_{task} . However, when the received data is, for example, a feature map, it requires semantic decoding and task operation based on an image, thus requiring τ_{task} . For complicated tasks, such as image retrieval and generation, we need to run generative models, e.g., latent diffusion models, by utilizing visual semantics as the conditioning. All types of semantics, except for the conventional transmission of the image itself, require the same process. After running generative models, the image generation task is terminated, but the retrieval task needs the search duration. Here, we exclude the search duration because it depends on the given database.

Hardware Configurations: We utilized a single NVIDIA L4 GPU and a 12-core Intel Xeon CPU @ 2.20GHz, the common configuration of personal computing devices for running visual tasks. Herein, to account for the case where the transmitter lacks parallel computing resources, we also consider the cases where semantic extraction is done solely on the CPU. On the other hand, for complex tasks such as image generation, we utilized a single A100 GPU, which can provide sufficient computing power to complete the task.

Simple Task Scenario: We first consider a scenario where a simple task, i.e., detection, is required on the receiver as a detection task can cover both classification and localization tasks. Here, we used the COCO dataset for the simulation. For the comparison, we considered methods described in [23], [24]. Note that methods [23], [24] require semantic

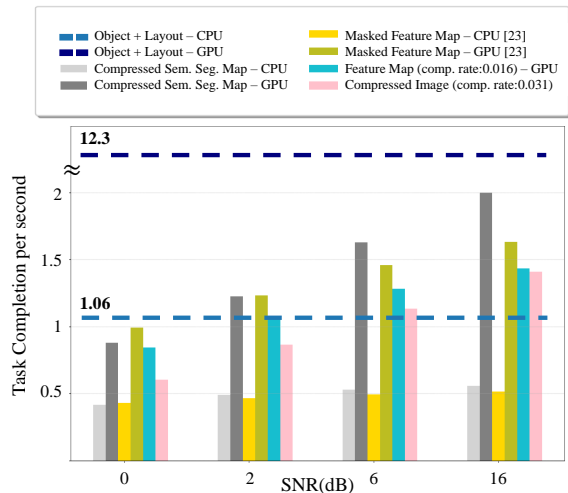


Fig. 11. Detection completion per second on different SNR regimes

decoding, i.e., image generation for task completion, as their semantics are hard to use directly on completing detection tasks. Specifically, [24] drops the object information from the semantic segmentation map; thus, reconstruction of objects is required, and [23] utilizes the feature map; thus, the decoding procedure is indispensable.

Fig. 11 shows the number of tasks completed per second under varying channel conditions. For clarity, methods that showed higher latency than naively transmitting the original image are not included in the figure. For example, [24] utilizes the pixel-level diffusion model [21], which consumes tens of seconds to generate a single image. For the semantic segmentation map-based method, we compressed it to the same level reported in [24] by down-sampling width and height. For image-based task completion, we utilized a detection model that demonstrates low τ_{task} [38].

The simulation results in Fig. 11 highlight the efficiency of our framework. With sufficient computing power at Tx, 12.3 tasks completion per second can be achieved, while other methods can complete under 2 tasks per second even at a high SNR regime. On the other hand, when Tx lacks its computational power, the framework still can manage 1.06 tasks per second, outperforming all other methods based on CPU in all SNR regimes. More importantly, task operation on compressed images or generated images potentially degrades performance. To analyze the trade-off between compression level and task performance of each method, average precision (AP) degradation along higher compression levels is measured. Here, AP is a representative performance measure for detection tasks. Fig. 12 shows the results tested on 1,000 COCO validation sets in 0dB SNR. The result shows that transmitting a compressed image can handle more images than ‘Object + Layout - CPU’ only when largely sacrificing its performance. Comparing a compressed feature map and a compressed image, the former achieves higher performance at the same speed when less compressed, but it largely degrades its performance along the higher compression. While we measured the latency of [24], as it generates a lower resolution

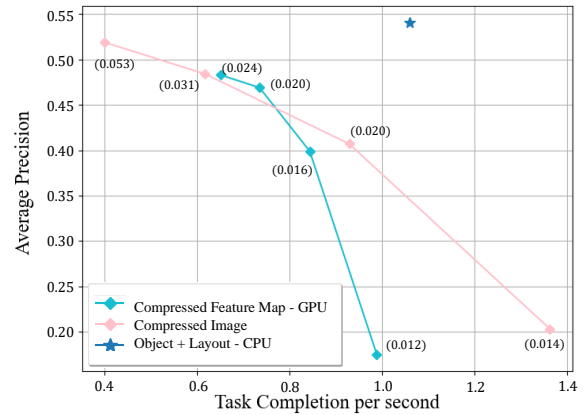


Fig. 12. Detection performance (average precision) v.s. task per second

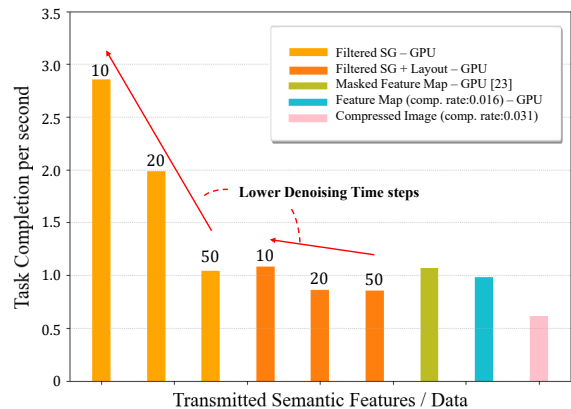


Fig. 13. Image generation completion per second for 0dB case

image than ours, we excluded it from measuring performance for fair comparison. Also, a segmentation map-based method can be easily expected to have a similar level of performance with ‘Object + Layout’ as it entails the same semantic features, although it showed low speed as depicted in Fig.11.

Complex Task Scenario: For more complex tasks such as image generation, simulation results are presented in Fig. 13. The results emphasize that the rapid delivery of semantic features is a critical factor impacting the number of task completions in a given time. Specifically, when generating a single image, using ‘Feature Map’ and ‘Masked Feature Map’ are significantly faster than employing ‘Filtered SG’ or ‘Filtered SG + Layout,’ which necessitates iterative denoising. However, in communication environments where various latency factors play, it is observed that even with LDM, a higher number of tasks per second can be achieved. Especially lowering denoising time steps to 10, ‘SG - GPU’ can deliver 4.6 times more images than ‘Compressed Image’.

V. CONCLUSION

In this paper, we suggest an efficient and effective semantic communication system for real-time CV tasks on the consideration of three key design points: **i)** Capability to select semantic features to transmit, **ii)** Filtering less informative semantic features to reduce transmitted bits, **iii)** Efficiently

utilizing the received semantic features to perform the task. In this sense, we thoroughly examine how much efficiency can be achieved by using compact visual semantics and how well the given CV tasks can be completed. Based on this study, we have analyzed the task performance for both simple and complicated tasks, demonstrating the impact of selective feature transmission on task performance. Our simulation results reveal that even with a minimal bit representation, compactly expressed semantic features can achieve sufficient task completion. Also, the simulations on limited bandwidth validate that task-adaptive selection of visual semantics is a possible enable for running real-time CV tasks.

ACKNOWLEDGMENTS

This work was supported by Institute of Information & communications Technology Planning & Evaluation (IITP) grant funded by the Korea government(MSIT) (No. RS2020-II201336, Artificial Intelligence Graduate School Program (UNIST)), and (No. IITP-2024-RS-2022-00156361, Innovative Human Resource Development for Local Intellectualization program), and the National Research Foundation of Korea (NRF) grant funded by the Korea government (MSIT) (No. RS-2024-00459023).

REFERENCES

- [1] W. Saad, M. Bennis, and M. Chen, "A vision of 6g wireless systems: Applications, trends, technologies, and open research problems," *IEEE network*, vol. 34, no. 3, pp. 134–142, 2019.
- [2] N. Panwar, S. Sharma, and A. K. Singh, "A survey on 5g: The next generation of mobile communication," *Physical Communication*, vol. 18, pp. 64–84, 2016.
- [3] D. C. Nguyen, M. Ding, P. N. Pathirana, A. Seneviratne, J. Li, D. Niyato, O. Dobre, and H. V. Poor, "6g internet of things: A comprehensive survey," *IEEE Internet of Things Journal*, vol. 9, no. 1, pp. 359–383, 2021.
- [4] M. Leo, G. Medioni, M. Trivedi, T. Kanade, and G. M. Farinella, "Computer vision for assistive technologies," *Computer Vision and Image Understanding*, vol. 154, pp. 1–15, 2017.
- [5] W. Yang, H. Du, Z. Q. Liew, W. Y. B. Lim, Z. Xiong, D. Niyato, X. Chi, X. Shen, and C. Miao, "Semantic communications for future internet: Fundamentals, applications, and challenges," *IEEE Communications Surveys & Tutorials*, vol. 25, no. 1, pp. 213–250, 2022.
- [6] Y. Tian, G. Pan, and M.-S. Alouini, "Applying deep-learning-based computer vision to wireless communications: Methodologies, opportunities, and challenges," *IEEE Open Journal of the Communications Society*, vol. 2, pp. 132–143, 2020.
- [7] W. Yang, H. Du, Z. Q. Liew, W. Y. B. Lim, Z. Xiong, D. Niyato, X. Chi, X. Shen, and C. Miao, "Semantic communications for future internet: Fundamentals, applications, and challenges," *IEEE Communications Surveys & Tutorials*, vol. 25, no. 1, pp. 213–250, 2022.
- [8] W. Weaver, *The mathematical theory of communication*. University of Illinois Press, 1963.
- [9] Z. Qin, X. Tao, J. Lu, W. Tong, and G. Y. Li, "Semantic communications: Principles and challenges," *arXiv preprint arXiv:2201.01389*, 2021.
- [10] X. Luo, H.-H. Chen, and Q. Guo, "Semantic communications: Overview, open issues, and future research directions," *IEEE Wireless Communications*, vol. 29, no. 1, pp. 210–219, 2022.
- [11] J. Bao, P. Basu, M. Dean, C. Partridge, A. Swami, W. Leland, and J. A. Hendler, "Towards a theory of semantic communication," in *2011 IEEE Network Science Workshop*, 2011, pp. 110–117.
- [12] P. Basu, J. Bao, M. Dean, and J. Hendler, "Preserving quality of information by using semantic relationships," *Pervasive and Mobile Computing*, vol. 11, pp. 188–202, 2014.
- [13] J. Liu, W. Zhang, and H. V. Poor, "A rate-distortion framework for characterizing semantic information," in *2021 IEEE International Symposium on Information Theory (ISIT)*. IEEE, 2021, pp. 2894–2899.
- [14] H. Seo, J. Park, M. Bennis, and M. Debbah, "Semantics-native communication via contextual reasoning," *IEEE Transactions on Cognitive Communications and Networking*, vol. 9, no. 3, pp. 604–617, 2023.
- [15] H. Xie, Z. Qin, G. Y. Li, and B.-H. Juang, "Deep learning enabled semantic communication systems," *IEEE Transactions on Signal Processing*, vol. 69, pp. 2663–2675, 2021.
- [16] E. Boursoulatzé, D. B. Kurka, and D. Gündüz, "Deep joint source-channel coding for wireless image transmission," *IEEE Transactions on Cognitive Communications and Networking*, vol. 5, no. 3, pp. 567–579, 2019.
- [17] A. Vaswani, "Attention is all you need," *Advances in Neural Information Processing Systems*, 2017.
- [18] D. B. Kurka and D. Gündüz, "Bandwidth-agile image transmission with deep joint source-channel coding," *IEEE Transactions on Wireless Communications*, vol. 20, no. 12, pp. 8081–8095, 2021.
- [19] C. Chaccour, W. Saad, M. Debbah, Z. Han, and H. V. Poor, "Less data, more knowledge: Building next generation semantic communication networks," *IEEE Communications Surveys & Tutorials*, 2024.
- [20] I. Goodfellow, J. Pouget-Abadie, M. Mirza, B. Xu, D. Warde-Farley, S. Ozair, A. Courville, and Y. Bengio, "Generative adversarial networks," *Communications of the ACM*, vol. 63, no. 11, pp. 139–144, 2020.
- [21] W. Wang, J. Bao, W. Zhou, D. Chen, D. Chen, L. Yuan, and H. Li, "Semantic image synthesis via diffusion models," *arXiv preprint arXiv:2207.00050*, 2022.
- [22] J. Ho, A. Jain, and P. Abbeel, "Denoising diffusion probabilistic models," in *Advances in Neural Information Processing Systems*, H. Larochelle, M. Ranzato, R. Hadsell, M. Balcan, and H. Lin, Eds., vol. 33. Curran Associates, Inc., 2020, pp. 6840–6851. [Online]. Available: https://proceedings.neurips.cc/paper_files/paper/2020/file/4c5bcfec8584af0d967f1ab10179ca4b-Paper.pdf
- [23] D. Huang, F. Gao, X. Tao, Q. Du, and J. Lu, "Toward semantic communications: Deep learning-based image semantic coding," *IEEE Journal on Selected Areas in Communications*, vol. 41, no. 1, pp. 55–71, 2022.
- [24] E. Grassucci, S. Barbarossa, and D. Comminiello, "Generative semantic communication: Diffusion models beyond bit recovery," *arXiv preprint arXiv:2306.04321*, 2023.
- [25] L. Qiao, M. B. Mashhadi, Z. Gao, C. H. Foh, P. Xiao, and M. Bennis, "Latency-aware generative semantic communications with pre-trained diffusion models," *arXiv preprint arXiv:2403.17256*, 2024.
- [26] M. Yang, D. Gao, F. Xie, J. Li, X. Song, and G. Shi, "Sg2sc: A generative semantic communication framework for scene understanding-oriented image transmission," in *ICASSP 2024-2024 IEEE International Conference on Acoustics, Speech and Signal Processing (ICASSP)*. IEEE, 2024, pp. 13 486–13 490.
- [27] M. U. Lokumarambage, V. S. S. Gowrisetty, H. Rezaei, T. Sivalingam, N. Rajatheva, and A. Fernando, "Wireless end-to-end image transmission system using semantic communications," *IEEE Access*, vol. 11, pp. 37 149–37 163, 2023.
- [28] X. Li, J. Shi, and Z. Chen, "Task-driven semantic coding via reinforcement learning," *IEEE Transactions on Image Processing*, vol. 30, pp. 6307–6320, 2021.
- [29] W. Zhang, Y. Wang, M. Chen, T. Luo, and D. Niyato, "Optimization of image transmission in cooperative semantic communication networks," *IEEE Transactions on Wireless Communications*, vol. 23, no. 2, pp. 861–873, 2023.
- [30] G. Zhang, Q. Hu, Z. Qin, Y. Cai, G. Yu, and X. Tao, "A unified multi-task semantic communication system for multimodal data," *IEEE Transactions on Communications*, 2024.
- [31] K. He, X. Zhang, S. Ren, and J. Sun, "Deep residual learning for image recognition," in *Proceedings of the IEEE conference on computer vision and pattern recognition*, 2016, pp. 770–778.
- [32] R. Rombach, A. Blattmann, D. Lorenz, P. Esser, and B. Ommer, "High-resolution image synthesis with latent diffusion models," in *Proceedings of the IEEE/CVF conference on computer vision and pattern recognition*, 2022, pp. 10 684–10 695.
- [33] Y. Cong, M. Y. Yang, and B. Rosenhahn, "Reltr: Relation transformer for scene graph generation," *IEEE Transactions on Pattern Analysis and Machine Intelligence*, vol. 45, no. 9, pp. 11 169–11 183, 2023.
- [34] N. Reimers, "Sentence-bert: Sentence embeddings using siamese bert-networks," *arXiv preprint arXiv:1908.10084*, 2019.
- [35] R. Krishna, Y. Zhu, O. Groth, J. Johnson, K. Hata, J. Kravitz, S. Chen, Y. Kalantidis, L.-J. Li, D. A. Shamma *et al.*, "Visual genome: Connecting language and vision using crowdsourced dense image annotations," *International journal of computer vision*, vol. 123, pp. 32–73, 2017.
- [36] T.-Y. Lin, M. Maire, S. Belongie, J. Hays, P. Perona, D. Ramanan, P. Dollár, and C. L. Zitnick, "Microsoft coco: Common objects in

- context,” in *Computer Vision–ECCV 2014: 13th European Conference, Zurich, Switzerland, September 6–12, 2014, Proceedings, Part V 13*. Springer, 2014, pp. 740–755.
- [37] O. Russakovsky, J. Deng, H. Su, J. Krause, S. Satheesh, S. Ma, Z. Huang, A. Karpathy, A. Khosla, M. Bernstein *et al.*, “Imagenet large scale visual recognition challenge,” *International journal of computer vision*, vol. 115, pp. 211–252, 2015.
- [38] N. Carion, F. Massa, G. Synnaeve, N. Usunier, A. Kirillov, and S. Zagoruyko, “End-to-end object detection with transformers,” in *European conference on computer vision*. Springer, 2020, pp. 213–229.
- [39] Y. Li, H. Liu, Q. Wu, F. Mu, J. Yang, J. Gao, C. Li, and Y. J. Lee, “Gligen: Open-set grounded text-to-image generation,” in *Proceedings of the IEEE/CVF Conference on Computer Vision and Pattern Recognition*, 2023, pp. 22 511–22 521.